Organic & Biomolecular Chemistry

Cite this: *Org. Biomol. Chem.*, 2012, **10**, 6309

www.rsc.org/obc

PAPER

Chemoenzymatic synthesis, structural study and biological activity of novel indolizidine and quinolizidine iminocyclitols†

Livia Gómez,[a] Xavier Garrabou,[a] Jesús Joglar,[a] Jordi Bujons,[a] Teodor Parella,[b] Cristina Vilaplana,[c] Pere Joan Cardona[c] and Pere Clapés*[a]

Received 16th May 2012, Accepted 14th June 2012
DOI: 10.1039/c2ob25943e

The synthesis, conformational study and inhibitory properties of diverse indolizidine and quinolizidine iminocyclitols are described. The compounds were chemo-enzymatically synthesized by two-step aldol addition and reductive amination reactions. The aldol addition of dihydroxyacetone phosphate (DHAP) to *N*-Cbz-piperidine carbaldehyde derivatives catalyzed by L-rhamnulose 1-phosphate aldolase from *Escherichia coli* provides the key intermediates. The stereochemical outcome of both aldol addition and reductive amination depended upon the structure of the starting material and intermediates. The combination of both reactions furnished five indolizidine and six quinolizidine type iminocyclitols. A structural analysis by NMR and *in silico* density functional theory (DFT) calculations allowed us to determine the population of stereoisomers with the *trans* or *cis* ring fusion, as a consequence of the inversion of configuration of the bridgehead nitrogen. The *trans* fusion was by far the most stable, but for certain stereochemical configurations of the 3-hydroxymethyl and hydroxyl substituents both *trans* and *cis* fusion stereoisomers coexisted in different proportions. Some of the polyhydroxylated indolizidines and quinolizidines were shown to be moderate to good inhibitors against α-L-rhamnosidase from *Penicillium decumbens*. Indolizidines were found to be moderate inhibitors of the rat intestinal sucrase and of the exoglucosidase amyloglucosidase from *Aspergillus niger*. In spite of their activity against α-L-rhamnosidase, all the compounds were ineffective to inhibit the growth of the *Mycobacterium tuberculosis*, the causative agent of tuberculosis.

Introduction

Polyhydroxylated indolizidines, *e.g.* D-swainsonine, castanospermine, lentiginosine, and steviamine (Fig. 1), and quinolizidines are conformationally restricted iminocyclitols. Several of them are effective glycosidase inhibitors and possess potential therapeutic applications as antidiabetic, antiviral, anticancer, antimetastatic and immunoregulating agents.[1–4]

Many efforts have been devoted to the chemical synthesis of polyhydroxylated indolizidine and quinolizidine iminocyclitols[5,6] as well as to evaluate their inhibitory properties against glycoprocessing enzymes.[3,4,7–10,11] However, few studies on the use of aldolases to construct stereoselectively the polyhydroxylated scaffold have been reported.[8]

We have recently reported that iminocyclitols of the pyrrolizidine type can be expediently prepared by an aldol addition reaction of DHAP to *N*-Cbz-pyrrolidine carbaldehyde derivatives from proline and 3- and 4-hydroxyproline derivatives catalyzed by L-rhamnulose-1-phosphate aldolase (RhuA) and the L-fuculose-1-phosphate aldolase F131A mutant (FucA F131A) in good yields.[12,13] This chemo-enzymatic approach has been demonstrated to be attractive for the diversity-oriented synthesis.[14]

The versatility of this methodology has led us to explore the chemo-enzymatic synthesis of polyhydroxylated indolizidines and quinolizidines in the frame of our ongoing project on the chemo-enzymatic synthesis of iminocyclitols. Our previous results prompted us to explore the use of *N*-Cbz-piperidine carbaldehyde derivatives as aldehyde acceptors to prepare novel polyhydroxylated indolizidine and quinolizidine iminocyclitols and test their preliminary biological activity as inhibitors of selected commercial glycosidases and rat intestinal disaccharide glycosidases. Inhibitors of digestive glycosidases decrease the post-prandial glycaemia by diminishing the rate of the digestion

[a]*Dept Biological Chemistry and Molecular Modeling, Instituto de Química Avanzada de Cataluña, IQAC-CSIC, Jordi Girona 18-26, 08034 Barcelona, Spain. E-mail: pere.clapes@iqac.csic.es*
[b]*Servei de Ressonància Magnètica Nuclear, Departament de Química, Universitat Autònoma de Barcelona, Bellaterra, Spain*
[c]*Unitat de Tuberculosi Experimental, Fundació Institut d'Investigació en Ciències de la Salut Germans Trias i Pujol, Edifici Laboratoris de Recerca, Crtra. de Can Ruti, Camí de les Escoles, s/n, 08916 Badalona, Spain*

†Electronic supplementary information (ESI) available. See DOI: 10.1039/c2ob25943e

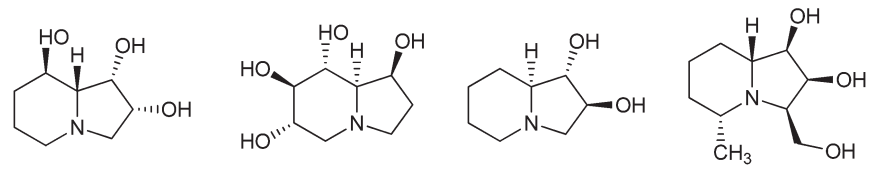

Fig. 1 Structures of biologically active indolizidine iminocyclitols.

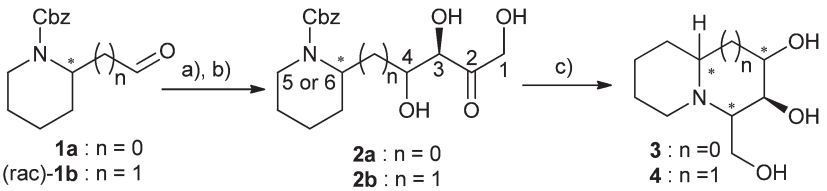

Scheme 1 Chemoenzymatic synthesis of indolizidines and quinolizidine analogues: (a) dihydroxyacetone phosphate (DHAP) and DHAP-dependent aldolase; (b) acid phosphatase, (c) H_2, Pd/C.

of dietary carbohydrates and, therefore, retarding the glucose absorption.[15,16] This is one of the therapeutic approaches to reduce the severity of diabetes mellitus type 2 and a way to prevent the metabolic syndrome associated with hypercaloric diets, provided that the inhibitor does not stimulate the insulin secretion.[17,18]

Results and discussion

We focused our attention on the commercial (*R*) or (*S*)-*N*-Cbz-piperidin-2-carbaldehyde ((*S*)-**1a** and (*R*)-**1a**) and *rac*-*N*-Cbz-2-(piperidin-4-yl)acetaldehyde ((*rac*)-**1c**) which are the starting aldehydes of choice for the key enzymatic aldol addition with DHAP (Scheme 1). DHAP dependent aldolases, investigated in previous work,[13] L-rhamnulose-1-phosphate aldolase (RhuA), L-fuculose-1-phosphate aldolase (FucA) wild type and the mutants FucA F131A, FucA F206A and FucA F206A/F131A, were selected as potential biocatalysts. FucA F131A was particularly effective as a catalyst for the aldol addition of DHAP to (*R*) and (*S*)-*N*-Cbz-prolinal derivatives, and therefore it may be also effective for the piperidine derivatives.[13] Both FucA F206A and F206A/F131A were also designed to accommodate sterically demanding aldehyde acceptors. Although they were not as effective as the single F131A mutant, we considered that they could be worth trying towards piperidine derivatives. The screening (Table 1) revealed that the FucA catalysts rendered scarce yields which were not satisfactory from a preparative point of view. RhuA gave the best results and was the selected aldolase to scale up the reactions (Table 2).

The aldol adducts (5*S*)-**2a**, (5*R*)-**2a**, **2b** (*i.e.* product mix from (*rac*)-**1b**) obtained were converted into the corresponding indolizidines and quinolizidines by one pot two-step *N*-Cbz-deprotection/reductive amination with H_2 (Scheme 1) in the presence of Pd/C, using the procedures previously published.[13] The iminocyclitols were purified by ion exchange chromatography, which rendered the pure compounds or mixtures of diastereomers (Table 2 and Fig. 2). From the structural analysis of the iminocyclitols thus obtained, it was inferred that the aldol addition of DHAP to (*S*)-**1a** catalyzed by RhuA furnished the *syn* configuration of the aldol adduct, (5*S*)-**2a**, which was consistent with the results obtained with (*S*)-*N*-Cbz-prolinal derivatives.[13] On the other hand, its enantiomer, (*R*)-**1a**, furnished the (5*R*)-**2a** adduct as a *syn* : *anti* 2 : 3 mixture. This was not observed in the case of the pyrrolidine derivative, (*R*)-*N*-Cbz-prolinal, which exclusively provided the *syn* adduct.[13] Both enantiomers of (*rac*)-**1b** yielded aldol adducts, (6*S*)-**2b** and (6*R*)-**2b**, as *syn* : *anti* mixtures, the *syn* configuration being the major diastereomers (Table 2). According to our previous observations, the reductive amination of polyhydroxylated pyrrolizidines gave preferentially the 3-hydroxymethyl and 1-hydroxy groups in a *syn* orientation.[13,14] In the present case, the reductive amination followed this trend for (5*R*)-**2a** and (6*R*)-**2b** adducts furnishing the corresponding indolizidines with a 6 : 1 *syn*(1*R*,3*R* or 1*S*,3*S*) : *anti* (1*R*,3*S*) ratio and the quinolizidines with an ~8 : 1 *syn* (2*S*,4*S*) : *anti*(2*S*,4*R* or 2*R*,4*S*) ratio, respectively with the major configuration consistent with the stereochemistry reported in previous studies. On the other hand, for (5*S*)-**2a** and (6*S*)-**2b** adducts the reductive amination was not (dia)stereoselective furnishing *syn* : *anti* mixtures with 1 : 1 and ~1 : 2 ratios, respectively.

Structural studies

Complete ^1H and ^{13}C chemical shift assignments for all derivatives **3a–e** and **4a–f** were performed by the aid of two-dimensional COSY and HSQC spectra. Furthermore, *J*(HH) coupling constants and NOESY data were required for the determination of the relative configuration of all stereogenic centers (see ESI† for detailed nOe contacts in each molecule). Another important question is whether a unique or several stereoisomers co-exist for each compound in solution. For the compounds considered in this work, *cis* and *trans* ring fusion can be achieved through inversion of the configuration at the bridgehead nitrogen with concomitant change of the conformation of the ring systems. In general, as it is known for decalin, most of them present a *trans* fusion that is energetically more stable. However, the

Table 1 Aldol addition reaction of dihydroxyacetone phosphate (DHAP) to *N*-Cbz-piperidinaldehyde derivatives (*S*)-**1a**, (*R*)-**1a** and (*rac*)-**1b**, catalysed by FucA and RhuA DHAP-dependent aldolases

Aldehyde	FucA % aldol adduct;[a] (*syn*(3*R*,4*S*) : *anti*(3*R*,4*R*))	FucA F131A	FucA F206A	FucA F131A/F206A	RhuA
(*S*)-**1a**	7[b]	19[b]	3[b]	18[b]	71; (>97 : 3)
(*R*)-**1a**	4[b]	21[b]	9[b]	18[b]	81; (40 : 60)
(*rac*)-**1b**	7[b]	15[b]	10[b]	12[b]	66; ([c])

[a] Percentage of aldol adduct formed with respect to the limiting substrate DHAP. The amount of aldol adduct was determined by HPLC using an external standard method. [b] *syn*(3*R*,4*S*) : *anti*(3*R*,4*R*) ratio not determined. [c] See Table 2.

Table 2 RhuA catalyzed synthesis of polyhydroxylated indolizidines and quinolizidines

Aldehyde	%[a]	Isolated yield %; aldol adduct	*syn*(3*R*,4*S*) : *anti*(3*R*,4*R*)[b]	Isolated indolizidine or quinolizidine	Isolated amount (mg)
(*S*)-**1a**	71	34; (5*S*)-**2a**	>97 : 3	**3a**	20
				3b	20
(*R*)-**1a**	81	32; (5*R*)-**2a**	40 : 60	**3c**	13
				3d	11
				3e	4
(*rac*)-**1b**	66	54[c]	64 : 36[d]	**4a**	17
				4b/**4c**/**4f** 70 : 21 : 9	17
				4c/**4b** 62 : 38	25
		(6*S*)-**2b** and (6*R*)-**2b**	87 : 13[e]	**4d**	47
				4e	3
				4f	3

Conversions, isolated yields and stereochemical outcome of the aldol additions of DHAP to *N*-Cbz-piperidinaldehyde derivatives and the corresponding isolated bicyclic products. [a] Percentage of aldol adduct formed in the reaction mixture determined by HPLC with respect to the limiting (DHAP) reagent. [b] *syn* : *anti* ratio for the RhuA-catalyzed aldol addition reaction. Inferred from the stereochemical analysis of the polyhydroxylated quinolizidine and indolizidine derivatives obtained. [c] The adducts corresponding to (6*S*)-**2b** and (6*R*)-**2b** from the aldol addition of DHAP to (*rac*)-**1b** were not separated by HPLC. [d] *syn* : *anti* ratio for the (6*S*)-**2b** adduct. [e] *syn* : anti ratio for the (6*R*)-**2b** adduct.

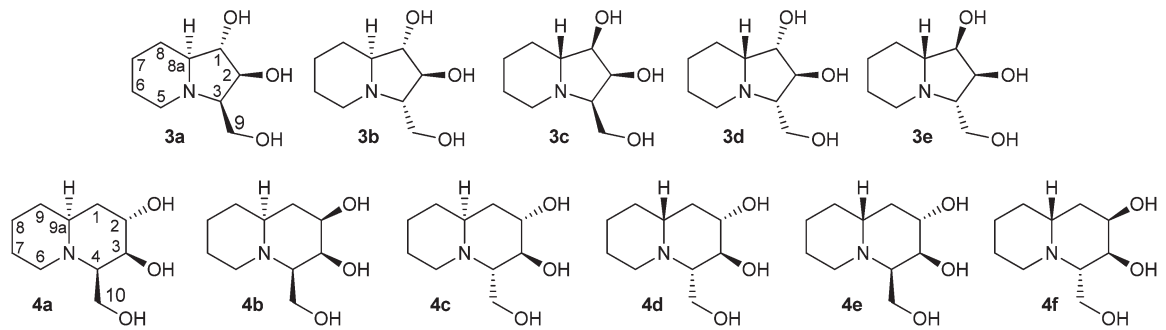

Fig. 2 Polyhydroxylated indolizidines and quinolizidines generated by enzymatic aldol addition, dephosphorylation and reductive amination steps.

pattern substitution and the relative configuration of the hydroxyl and hydroxymethylene groups play an important role to understand the conformational aspects of the five- or six-membered rings and to know the existence of different *cis–trans* fused stereoisomers.

^{1}H NMR spectra of the different indolizidine derivatives **3a–e** showed clear signals at room temperature. Two sets of stereoisomeric-related compounds (**3a**/**3d**/**3e** *vs.* **3b**/**3c**) were distinguished that could be correlated from the relative *cis*/*trans* configuration between the C3 and C8a stereocenters. Thus, distinctive upfield effects on H8a and H3 chemical shifts owing to their well-defined axial positions, high diastereotopicity for the two H5 methylene protons ($\Delta\delta$ = 1.1 ppm *vs.* 0.2/0.3 ppm) owing to well-defined axial–equatorial positions, and characteristic downfield effects on the methylene C5 chemical shift were clearly observed for the **3a**/**3d**/**3e** compounds, which practically exist as a single *trans* stereoisomer (see ESI Table S1†). Otherwise, the relative configuration of the C1–C2–C3 centers could be determined from their corresponding chemical shift values as well as from the characteristic nOe data (see ESI†). On the other hand, compounds **3b** and **3c** present relevant chemical shift differences for H8a, H3, H5 protons and for the C5 carbon (see ESI Table S1†). In addition, characteristic nOe data evidenced the presence of different *cis*/*trans* states in fast equilibrium on the NMR timescale, in quite good agreement with theoretical calculations (see below).

^{1}H NMR spectra of the different quinolizidine derivatives **4a–f** also show clear signals at room temperature except for **4e** that shows some broad signals due to some slow dynamic equilibria on the NMR timescale. In all these compounds, the well-defined chair conformation related to a six-membered ring allows a more simple analysis of chemical shifts and *J*(HH) values. The relative configuration of the C2/C3/C4 is easily determined from *J*(HH) and nOe data (see ESI†). Large axial–axial *J*(HH) values (8–9 Hz) and characteristic 1,3-diaxial nOe contacts among others confirm the axial position whereas smaller *J*(HH) values and the absence of 1,3-diaxial nOe contacts confirm the equatorial position of H2/H3/H4 protons. In addition, the relative configuration of the C4 center is determined in all compounds from the hydroxymethyl C10 chemical shift as well as from key nOe contacts (see ESI Table S2 and Fig. S1–S12†). Exclusive *trans* stereoisomers are clearly determined for compounds **4a**, **4b**, **4d** and **4f** whereas important contributions of the *cis* stereoisomer must be effective for **4c** and **4e**. As discussed above, there is a strong correlation between the relative configurations of C4 and C9a centers in *trans* fused products as observed from the following experimental NMR data (see ESI Table S2†): (i) a notorious upfield effect on H9a and H4 chemical shifts, (ii) a high diastereotopicity for the two H6 methylene protons owing to a clear axial–equatorial position, and (iii) characteristic C6 and C9 chemical shifts. All these experimental aspects are also in strong agreement with theoretical calculations (see below).

To corroborate the NMR results, an *in silico* conformational analysis of compounds **3a–e** and **4a–f** was carried out by using density functional theory (DFT) calculations (see ESI†). Two additional model compounds, 1-deoxy-castanospermine (DOC) and 1-deoxy-8a-*epi*-castanospermine (DOEC), which have been reported to exist as $^8C_5$ and $^5C_8$ stereoisomers in solution,[19] were also analyzed to assess the suitability of the method used. The results for these model compounds were in good agreement with the experimental observations, showing that all DOC minima detected showed *trans*-fused $^8C_5$ geometry, while for DOEC an 8 : 2 *trans*-$^5C_8$: *cis*-$^8C_5$ ratio was estimated (Table 3). Furthermore, among the indolizidines synthesized in this work, significant populations of *cis*-fused stereoisomers were only determined for compounds **3b** and **3c**, while **3a**, **3d** and **3e** yielded exclusively *trans*-fused ones (Table 3, Fig. 3 and ESI Table S3, Chart S1 and Fig. S15†). On the other hand, among the quinolizidines, only **4c** and **4e** showed a significant contribution of *cis*-fused stereoisomers. Thus, the theoretical results obtained support the analysis of the NMR data of the compounds synthesized.

Table 3 Relative population of *trans* and *cis* stereoisomers in water solution for compounds **3a–e**, **4a–f**, 1-deoxycastanospermine (DOC) and 1-deoxy-8a-*epi*-castanospermine (DOEC) determined from DFT calculations and calculated as the sum of Boltzmann contributions of the stereoisomers of each type

Compound	*trans* (%)	*cis* (%)
3a	100	
3b	73.2	26.8
3c	56.9	43.1
3d	100	
3e	100	
4a	100	
4b	100	
4c	48.6	51.4
4d	100	
4e	96.4	3.6
4f	100	
DOC	100	
DOEC	81.0	19.0

Inhibitory activity against glycosidases, rat intestinal disaccharidases and endo/exoglucosidases. The polyhydroxylated indolizidines **3a–e** and quinolizidines **4a–f** synthesized were tested as inhibitors against commercial glycosidases (Table 4) and rat intestinal disaccharidases (Table 5) as preliminary targets for inhibition. Their activity was compared with the known glycosidase inhibitors 1,4-dideoxy-1,4-imino-D-arabinitol (DAB1, **8**), 1,4-dideoxy-1,4-imino-L-arabinitol (LAB1, **9**), D-fagomine (**10**) and L-fagomine (**11**) (Fig. 4). D-Fagomine (**10**) effectively lowers blood glucose in a dose-dependent manner when ingested together with sucrose or starch, without stimulating insulin secretion.[15]

Indolizidines. Compounds **3a–e** can be considered ring extended analogues of the pyrrolidines **8** and **9** (Fig. 4) but also analogues of lentiginosine and swainsonine (Fig. 1).[9,20] Lentiginosine was a selective inhibitor of amyloglucosidases from *Aspergillus niger* and *Rhizopus* mold but does not inhibit rat intestinal sucrase and maltase as well as α-D-glucosidase from Baker's yeast, β-D-glucosidase from almonds and *A. niger* and α-D-mannosidase from jack beans.[21] Swainsonine is a strong inhibitor of α-D-mannosidase from different origins (IC_{50} = 0.1 μM, against α-D-mannosidase from jack beans).[2,20]

Interestingly, we found that compounds **3a** and **3e** are selective inhibitors of α-L-rhamnosidase from *Penicillium decumbens*, while **3c** was found to inhibit also α-D-mannosidase and moderately, α-L-fucosidase (Table 4). Product **3b** was also found to be a weak inhibitor of α-D-glucosidase from Baker's yeast. Among the indolizidines synthesized in this work, **3a** was the most potent inhibitor (Table 4) of α-L-rhamnosidase. Because **3a** has no activity with the other commercial glycosidases tested (Table 4) nor against rat intestinal glycosidases (see below, Table 5), this may indicate a highly selective inhibitor of α-L-rhamnosidase. Changing the configuration of any stereogenic centre resulted in a loss of inhibitory properties.

Regarding the inhibitory properties against rat intestinal glycosidases, **3b**, **3c**, and **3e** are selective inhibitors of rat intestinal sucrase (Table 5). Interestingly, **3b** has an IC_{50} against sucrase comparable to DAB1 (**8**) and lower than that of D- and L-fagomine. D-Fagomine effectively lowers the postprandial glycaemia and therefore compound **3b** is a promising analogue with a potential application in controlling blood glucose levels.

Quinolizidines. The polyhydroxylated quinolizidines **4a–f** can also be considered ring extended analogues of **10** and **11**. They can also be seen as deoxy analogues of quinolizidine (**12**) (Fig. 3), which was reported by Liu *et al.*[7] and it was found to be a potent inhibitor of α-D-glucosidase I from pig kidney (IC_{50} = 0.15 μM).

Interestingly, among the quinolizidines, only **4e** and **4f** were found to be selective inhibitors of α-L-rhamnosidase (Table 4). Moreover, **4a** and **4d** were selective but weak inhibitors of rat

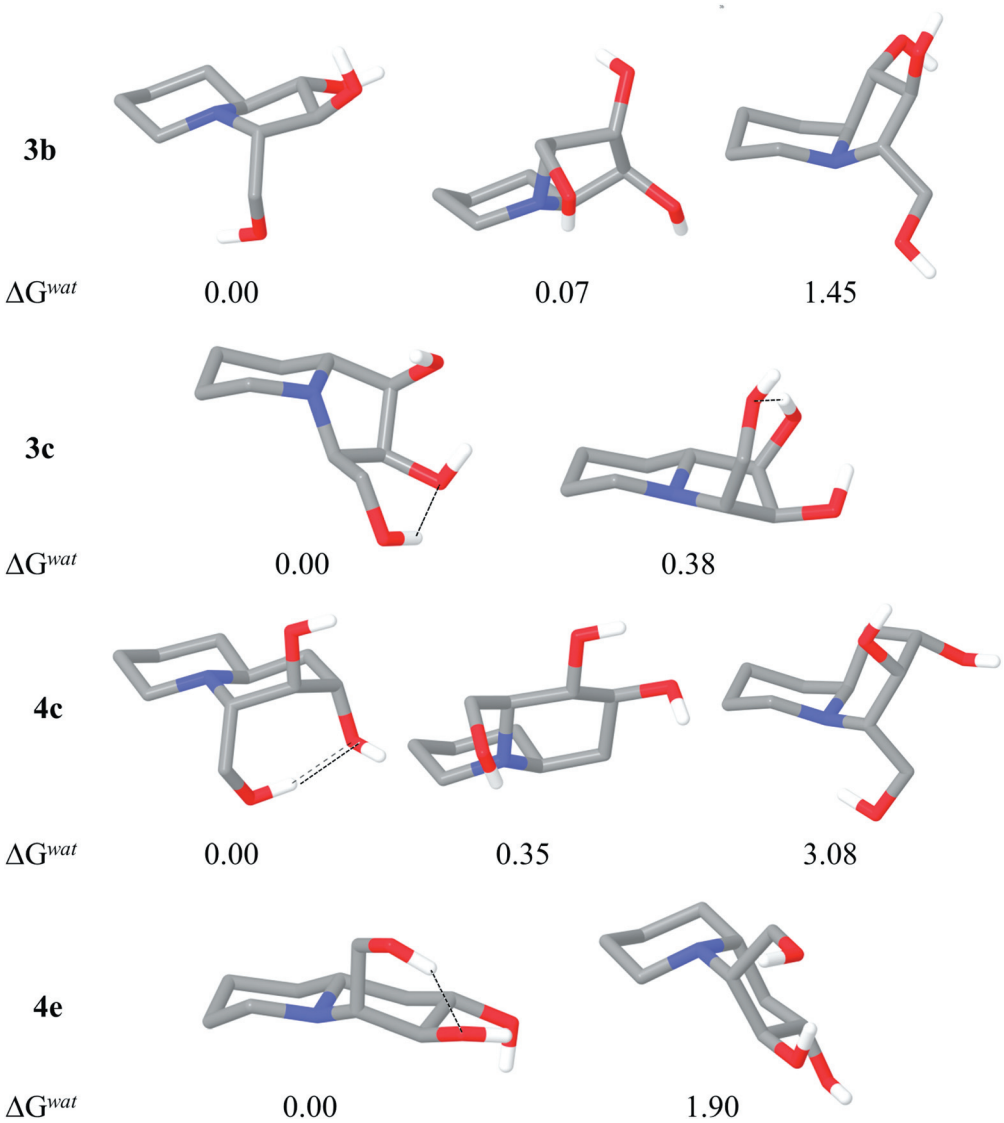

Fig. 3 Minimum energy *cis*/*trans*-stereoisomers determined for compounds **3b**, **3c**, **4c** and **4e**, and relative Gibbs free energies in water solution (ΔG^{wat}, kcal mol^{-1}) estimated through density functional theory calculations at B3LYP/cc-pVTZ(-f) level.

intestinal sucrase (Table 5). The rest of the compounds showed no inhibitory activity against both the selected commercial glycosidases and the rat intestinal disaccharidases tested. Most of the quinolizidines described in the literature are either weak inhibitors or inactive against the most common commercial glycosidases.[4,11]

Inhibitory properties against endo and exoglucosidases. The indolizidines and quinolizidines were also assayed as inhibitors of the endoglucosidase α-amylase from human saliva and porcine pancreas.[6,23] Two substrates were used: starch and the chromophore-tagged starch-azure.[24] The compounds synthesized, including the parent DAB1 (**8**), LAB1 (**9**), D-fagomine (**10**) and L-fagomine (**11**), were inactive against the α-amylases. The amyloglucosidase from *A. niger* was selected as *exo*glucosidase using *p*-nitrophenyl glucopyranoside as the substrate. Among the parent compounds, DAB1 (**8**) was the most potent inhibitor while **9**, **10** and **11** were moderate to weak inhibitors of amyloglucosidase, the D-series of these iminocyclitols being more potent than the corresponding L-ones (Table 6). Among the indolizidines, **3d** had moderate activity, comparable to LAB1 (**9**) and D-fagomine (**10**), while compounds **3a** and **3b** were >10-fold less active (Table 6). Interestingly, **3a** and **3b** are 3-hydroxymethyl analogues of (+)-lentiginosine, which is a potent and selective inhibitor of *A. niger* amyloglucosidase (K_i = 2 μM[9]). Thus, the introduction of a hydroxymethyl substituent with *R*/*S*-configuration at C-3 of (+)-lentiginosine leads to a strong decrease of its activity. However, this effect is partially reverted if the (3*S*)-hydroxymethyl substitution is combined with the epimeric configuration at C-8a (*i.e.* **3d**). On the other hand, no activity was observed with the quinolizidines synthesized.

Inhibition of the glucose release from starch hydrolysis. We explore the ability of the compounds synthesized to inhibit the release of glucose from the hydrolysis of starch by the gut mucosal suspension from rat intestine. In this case starch can be

Table 4 Activities, IC_{50} (μM) and K_i (μM) (in parenthesis), of the compounds synthesized against commercial glycosidases[a]

Compound	α-D-Glucosidase[b]	α-D-Glucosidase[c]	β-D-Glucosidase[d]	β-D-Galactosidase[e]	α-L-Rhamnosidase[f]	α-D-Mannosidase[g]	α-L-Fucosidase[h]
8[i]	0.33 ± 0.02 (0.17 ± 0.01) C	61 ± 7 (104 ± 75) C	276 ± 25 (100 ± 64) C	n.i.	n.i.	286 ± 27 (111 ± 60) NC, α > 1	20 ± 1 (5 ± 1) C
9[i]	1.8 ± 0.1 (0.8 ± 0.1) NC, α = 1	0.05 ± 0.01 (0.04 ± 0.01) NC, α > 1	685 ± 112 (1014 ± 81) NC, α > 1	n.i.	56 ± 5 (98 ± 5) NC, α = 1	n.i.	n.i.
10[i]	n.i.	126 ± 7 (236 ± 61) C	n.i.	154 ± 22 (76 ± 21) C[i]	n.i.	n.i.	n.i.
11[i]	n.i.	61 ± 7 (18 ± 8) C	n.i.	n.i.	n.i.	n.i.	n.i.
3a	n.i.	n.i.	n.i.	n.i.	3.3 ± 0.2 (3.0 ± 0.8) NC, α = 1	n.i.	n.i.
3b	n.i.	237 ± 68 (229 ± 44) C	n.i.	n.i.	113 ± 30 (84 ± 9) NC, α = 1	n.i.	n.i.
3c	n.i.	n.i.	n.i.	n.i.	35 ± 2 (21 ± 2) C	82 ± 9 (89 ± 1) C	593 ± 86 (135 ± 28) C
3e	n.i.	n.i.	n.i.	n.i.	55 ± 4 (52 ± 3) C	n.i.	n.i.
4e	n.i.	n.i.	n.i.	n.i.	26 ± 5 (17 ± 2) C	n.i.	n.i.
4f	n.i.	n.i.	n.i.	n.i.	85 ± 24 (76 ± 7) C	n.i.	n.i.

[a] Data are means of triplicate experiments ± standard error of the mean (SE). [b] From Baker's yeast. [c] From rice. [d] From sweet almonds. [e] From bovine liver. [f] From *Penicillium decumbens*. [g] From jack beans, *Genus canavalia*. [h] From bovine kidney. [i] Data from ref. 13. C: competitive inhibition. NC: non-competitive inhibition.[22] n.i. no inhibition, that is $IC_{50} \geq 1$ mM.

Table 5 IC_{50} (μM) values of the compounds synthesized against rat intestinal disaccharide glycosidases[a]

Compound	Sucrase	Lactase	Trehalase	Maltase
8[b]	22 ± 12	140 ± 84	67 ± 19	50 ± 36
9[b]	0.29 ± 0.02	50 ± 36	74 ± 34	0.2 ± 0.1
10[b]	144 ± 26	n.i.	n.i.	n.i.
11[b]	484 ± 4	n.i.	n.i.	209 ± 92
3b	62 ± 3	n.i.	n.i.	293± 19
3c	207 ± 44	n.i.	n.i.	n.i.
3e	117 ± 6	n.i.	n.i.	n.i.
4a	339 ± 266	n.i.	n.i.	n.i.
4d	824 ± 288	n.i.	n.i.	n.i.
Activity (UI)[c]	4.01 ± 0.48	0.75 ± 0.07	2.44 ± 0.41	27.50 ± 3.55

[a] The experiments were performed in triplicate for each set of disaccharide glycosidases obtained from one rat. Two different rats (n = 2) were used. Activities are expressed as μM ± standard error of the mean (SE). [b] Data from ref. 13. [c] Definition of activity: 1 U corresponds to 1 μmol of glucose formation per hour at 37 °C in phosphate buffer, pH 6.8. n.i. no inhibition, $IC_{50} \geq 1$ mM.

hydrolysed by the amylases and amyloglucosidases releasing glucose and other reducing oligosaccharides, which can be further hydrolysed by the presence of disaccharidases.[18] The Dahlqvist methodology[25] was employed to measure the glucose formed and therefore the activity was determined as the rate of glucose formation (Table 6). Among the parent compounds, LAB1 (**9**) was found to be a strong inhibitor of the glucose release from starch followed by DAB1 (**8**), which had good inhibitory properties. D-Fagomine (**10**) was a moderate inhibitor whereas its enantiomer, **11**, was only a weak inhibitor. Among the compounds synthesized, only the indolizidine **3b** was found to be a weak inhibitor, with an activity comparable to that of L-fagomine (**11**). The inhibition of glucose released from the starch hydrolysis is consistent with the observed disaccharidase inhibition (Table 5): DAB1 (**8**) and LAB1 (**9**) inhibited all the intestinal disaccharidases assayed whereas L-fagomine (**11**) was a weak inhibitor of sucrase and maltase, D-fagomine (**10**) being a weak inhibitor of sucrase. Compound **3b** was comparable to L-fagomine and did not correlate well with the observed activities against intestinal disaccharidases and amyloglucosidase from *A. niger*.

Inhibitory activity against *Mycobacterium tuberculosis* H37Rv laboratory strain. The L-rhamnopyranosyl moiety is present in a disaccharide linker between the arabinogalactan polysaccharide and peptidoglycan regions of the cell wall of *Mycobacterium tuberculosis*, the causative agent of tuberculosis.[26,27] Therefore inhibitors either of thymidine diphosphate-(dTDP)-rhamnose biosynthesis from dTDP-glucose or of incorporation of L-rhamnose into the mycobacterial cell wall may have potential as novel chemotherapeutic agents for the treatment of mycobacterial infection.[27,28] It has been suggested that iminocyclitol derivative inhibitors of α-L-rhamnosidase from *P. decumbens* could have

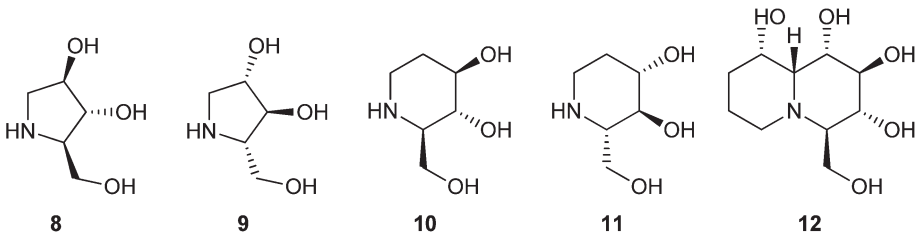

Fig. 4 Structures of polyhydroxylated pyrrolidine and piperidine iminocyclitols with known glycosidase inhibitory properties, analogues of the indolizidines **3a–e** and quinolizidines **4a–f**.

Table 6 Activities of the parent and synthesized compounds as inhibitors of amyloglucosidase from *Aspergillus niger* and as inhibitors of the glucose release from the hydrolysis of starch by the rat intestinal mucosa

Compound	Amyloglucosidase *A. niger* IC_{50} (μM)	Intestinal mucosa[a] IC_{50} (μM)[b]
8	6.7 ± 1.8	15.4 ± 2.1
9	43 ± 14	0.34 ± 0.03
10	27 ± 3	78 ± 13
11	98 ± 11	160 ± 30
3a	366 ± 29	n.i.
3b	347 ± 145	237 ± 51
3d	26 ± 9	n.i.

[a] Activity (U) = 20.8 ± 2.4. Definition of activity: 1 U corresponds to 1 μmol of glucose formation per hour at 37 °C in phosphate buffer pH 6.8. [b] IC_{50}: concentration of the compound that is required for 50% reduction of the rate of glucose released per hour.

the ability to inhibit dTDP-L-rhamnose biosynthesis and therefore the bacterial growth.[27] Compounds **3a**, **3e**, **4e** and **4f** were good inhibitors of rhamnosidase, and thus they were assayed in mycobacterial systems. However, no differences were found between the positive growth control experiment and the one in the presence of **3a**, **3b**, **3c**, and **3e** at 3 mg mL^{-1}, or **4e** and **4f** at 0.75 mg mL^{-1}. The minimal inhibitory concentration (MIC) (*i.e.* the lowest drug concentration that prevented the development of color akin to the bacterial growth) of LAB1 (**9**) was 2.5 mg mL^{-1}. As a reference, the MIC value found for isoniazid in this assay was 0.25 μg mL^{-1}, which is in good agreement with the reported values.[29]

Conclusions

We have developed a new strategy based on RhuA catalysis for the diversity-oriented synthesis of polyhydroxylated indolizidine and quinolizine iminocyclitols in two steps. The key reaction was the aldol addition of DHAP to *N*-Cbz-piperidin-2-carbaldehyde ((*S*)-**1a** and (*R*)-**1a**) or *rac*-*N*-Cbz-2-(piperidin-4-yl)acetaldehyde ((rac)-**1b**). Structural analysis of indolizidines **3a–e** and quinolizidines **4a–f** by means of NMR and *in silico* density functional theory (DFT) calculations showed populations of stereoisomers with *trans* or *cis* ring fusion, because of the inversion of configuration of the bridgehead nitrogen, that depends upon the stereochemistry of the hydroxymethyl and hydroxyl substituents. For instance, the indolizidine series **3a**, **3d** and **3e** showed exclusively a *trans* fused stereoisomer, whereas for **3b** and **3c** both *trans* and *cis* coexisted. Interestingly **3b** and **3c** possess a *syn* configuration (*i.e.* 3*S*,8a*S* or 3*R*,8a*R*, respectively) between H8a and the 3-hydroxymethyl group. Similarly, in the quinolizidine series, **4c** and **4e** showed a coexistence of *trans*/*cis* fused stereoisomers while the *trans* was the most predominant for the rest. Indolizidines **3a–c** and **3e** and quinolizidines **4e** and **4f** are good inhibitors of α-L-rhamnosidase from *P. decumbens*. Among them, **3a** was the most potent and selective inhibitor of α-L-rhamnosidase synthesized in this work. Concerning the inhibitory properties of rat intestinal disaccharidases, **3b** has an activity comparable to LAB and higher than D-fagomine (**10**), a compound that effectively lowers postprandial glycaemia.[15] Regarding the activity against the exoglucosidase amyloglucosidase from *A. niger*, the indolizidine **3d** has inhibitory properties comparable to DAB1 and D-fagomine, being the most active among the compounds synthesized. However, **3d** was a weak inhibitor of the glucose release from the hydrolysis of the starch by intestinal mucosa, which did not correlate well with its inhibitory properties against rat intestinal disaccharidases and amyloglucosidase. Although **3a–c** and **3e** and quinolizidines **4e** and **4f** are good inhibitors of α-L-rhamnosidase, they did not show any activity against the *M. tuberculosis* H37Rv laboratory strain. Therefore, in this case no correlation was found between both activities.

Experimental section

Materials synthesis

Dihydroxyacetone phosphate (DHAP) was obtained from the cyclic dimer precursor 2,5-diethoxy-*p*-dioxane-2,5-dimethanol-*O*-2^1-*O*-5^1-bisphosphate, which was synthesized in our lab using a procedure described by Jung *et al.*[30] with slight modifications. DHAP is released from the precursor by acidic hydrolysis at 65 °C. *N*-Cbz-amino aldehydes used in these studies were synthesized in our lab using procedures published in previous work.[13] L-Rhamnulose-1-phosphate aldolase [Co^{II}] (RhuA) (3.8 U mg^{-1}) (1 U catalyzes the cleavage of 1 μmol of L-rhamnulose-1-phosphate per minute at 25 °C and pH 7.5 (100 mM Tris·HCl + 150 mM KCl)),[31] L-fuculose-1-phosphate aldolase (FucA) (9.8 U mg^{-1}) protein and mutants FucA F131A (0.1 U mg^{-1}), FucA F206A (0.22 U mg^{-1}) and FucA F131A/F206A (<0.005 U mg^{-1}) were obtained as previously described (1 U cleaves 1 μmol of L-fuculose-1-phosphate per minute at 25 °C and pH 7.5 (100 mM Tris·HCl + 150 mM KCl)).[13,32] 1,4-Dideoxy-1,4-imino-D-arabinitol (DAB1, **8**), 1,4-dideoxy-1,4-imino-L-arabinitol (LAB1, **9**), D-fagomine (**10**) and L-fagomine

(**11**) were synthesized following the procedures developed by us and described in previous work.[33] Aqueous borate solutions were prepared by adjusting the desired pH of a solution of boric acid with 2 M aq. NaOH. Acid phosphatase (PA, EC 3.1.3.2, 5.3 U mg^{-1}) was from Sigma-Aldrich. All other solvents used were of analytical grade.

Biological activity

Ketamine chlorhydrate, Imalgene 1000, was from Merial Laboratorios S.A. (Barcelona, Spain), xylacine, Rompun 2%, was from Química Farmacéutica S.A. (Barcelona, Spain). Starch from potatoes, starch azure, 4-hydroxybenzoic acid, 4-aminoantipyrine, glucose oxidase type II-S from *Aspergillus niger*, peroxidase type II from horseradish, α-D-glucosidase from Baker's yeast; α-D-glucosidase from rice; β-D-glucosidase from sweet almonds; β-D-galactosidase from bovine liver; α-D-mannosidase from jack beans, *Genus Canavalia*; α-L-rhamnosidase from *Penicillium decumbens*, α-L-fucosidase from bovine kidney, α-amylase from porcine pancreas type I-A, α-amylase from human saliva type XIIIA and amyloglucosidase from *Aspergillus niger* and the synthetic substrates *p*-nitrophenyl-α-D-glucopyranoside, *p*-nitrophenyl-β-D-glucopyranoside, *p*-nitrophenyl-β-D-galactopyranoside, *p*-nitrophenyl-α-D-mannopyranoside, *p*-nitrophenyl-α-D-rhamnopyranoside, *p*-nitrophenyl-α-D-fucopyranoside were purchased from Sigma-Aldrich. Water for analytical and preparative HPLC and for the preparation of buffers and other assay solutions was obtained from an Arium® Pro Ultrapure Water Purification System (SartoriusStedim Biotech). All other solvents used were of analytical grade.

NMR spectroscopy. All NMR experiments were collected at 298 K in D_2O solutions on a Bruker Avance DRX-500 NMR instrument operating at 500.13 MHz for ^1H and at 125.77 MHz for ^{13}C, equipped with a TXI cryoprobe with only *Z*-gradients. Conventional 1D ^1H and 1D ^{13}C, selective 1D TOCSY and selective 1D NOESY and 2D COSY, 2D HSQC, 2D multiplicity-edited HSQC and 2D NOESY experiments were collected using standard Bruker software and acquired under routine conditions.

HPLC analyses. HPLC analyses were performed on an RP-HPLC cartridge, 250 × 4 mm filled with Lichrosphere® 100, RP-18, 5 μm (Merck) or on an RP-HPLC XBridge® C18, 5 μm, 4.6 × 250 mm column (Waters). Samples (25 μL) were withdrawn from the aldol reactions, dissolved in MeOH (1 mL) to stop the reaction and analysed by HPLC. The solvent system used was solvent (A) 0.1% (v/v) trifluoroacetic acid (TFA) in H_2O and solvent (B) 0.095% (v/v) TFA in ACN–H_2O 4 : 1, gradient elution from 30% to 90% B over 30 min, flow rate 1 mL min^{-1}, detection 215 nm, column temperature 30 °C. The amount of aldol adduct produced was quantified from the peak areas using an external standard methodology.

Preparation of *N*-Cbz-aminoaldehydes

(*R*)-*N*-(Benzyloxycarbonyl)-2-formylpiperidine ((*R*)-1a). (*R*)-*N*-(Benzyloxycarbonyl)pipecolic acid (5.0 g, 19.0 mmol) was dissolved in MeOH (20 mL) and the mixture was cooled down to 0 °C with an ice bath. To this solution, SO_2Cl_2 (76.3 mmol, 5.56 mL) was added dropwise at such a rate as to maintain the reaction mixture below 4 °C. Stirring of the reaction mixture was continued at room temperature overnight. Then, the solvent was removed under reduced pressure and the solid obtained washed with ethyl ether (5.1 g, 18.4 mmol, 97%). The methyl ester derivative (2.0 g, 7.2 mmol) was reduced by treatment with $NaBH_4$ (147.5 mmol, 5.6 g) using the procedure described by Luly *et al.* (method B) with slight modifications.[34] After the addition of $NaBH_4$ the reaction was allowed to warm up slowly until room temperature. The *N*-Cbz-aminoalcohol (1.5 g, 6.1 mmol) was oxidized by treatment with iodoxobenzoic acid (IBX)[35] using the procedures already described by us.[12,14] NMR spectra matched those previously published.[36] $[\alpha]_D^{22}$ = +23.8 (*c* 1.0 in $CHCl_3$). ^1H NMR (300 MHz, $CDCl_3$) δ 9.60 (s, 1H), 7.35 (m, 5H), 5.16 (s, 2H), 4.71 (d, J = 19.3 Hz, 1H), 4.10 (m, 1H), 3.73 (m, 1H), 3.53 (m, 1H), 2.95 (m, 1H), 2.22 (m, 1H), 1.65 (m, 1H), 1.40 (m, 1H), 1.26 (m, 1H). ^{13}C NMR (75 MHz, $CDCl_3$) δ 200.8, 136.3, 128.4, 128.0, 127.8, 67.4, 61.0, 42.6, 42.4, 24.5, 23.3, 20.7. HRMS-ESI: *m*/*z* calcd for $C_{14}H_{18}NO_3$ 248.1281 [M + H^+]; found 248.1275. This material was used directly in the next step without any further purification.

(*S*)-*N*-(Benzyloxycarbonyl)-2-formylpiperidine ((*S*)-1a). The title compound was prepared according to the procedure described above. Similar yield and identical NMR spectra and HRMS-ESI to that of the *R* enantiomer were obtained.[37] $[\alpha]_D^{22}$ = −26.5 (*c* 1.0 in $CHCl_3$). This material was used directly in the next step without any further purification.

***N*-Benzyloxycarbonyl-2-(2-oxoethyl)-piperidine (*rac*-1b).** To a solution of 2-(2-hydroxyethyl)piperidine (51.1 mmol, 6.60 g) in dioxane–water 4 : 1 (100 mL), Cbz-OSu (51.0 mmol, 12.7 g) in dioxane–water 4 : 1 (50 mL) was added dropwise at 25 °C. After stirring for 24 h, the mixture was evaporated to dryness under reduced pressure. The residue was dissolved with ethyl acetate (150 mL) and washed successively with 5% w/v aq. citric acid (3 × 50 mL), 10% w/v aq. $NaHCO_3$ (3 × 50 mL) and brine (2 × 50 mL). After drying over Na_2SO_4, the organic layer was evaporated under reduced pressure affording a white solid of *N*-Cbz-2-(2-hydroxyethyl)piperidine (47.5 mmol, 12.5 g, 93%). Oxidation of *N*-Cbz-2-(2-hydroxyethyl)piperidine (15.2 mmol, 4.0 g) was efficiently carried out by treatment with iodoxobenzoic acid (IBX),[35] affording the title compound (14.6 mmol, 3.8 g, 96%) as a colorless oil. NMR spectra matched those previously published.[38] ^1H NMR (300 MHz, $CDCl_3$) δ 9.70 (s, 1H), 7.33 (m, 5H), 5.11 (s, 2H), 4.92 (m, 1H), 4.09 (dd, J = 13.5, 9.7 Hz, 1H), 2.83 (td, J = 12.5, 8.8 Hz, 1H), 2.72 (dd, J = 8.0, 2.9 Hz, 1H), 2.59 (ddd, J = 15.7, 6.7, 2.1 Hz, 1H), 1.58 (m, 6H). ^{13}C NMR (75 MHz, $CDCl_3$) δ 200.5, 155.1, 136.5, 128.4, 127.9, 127.8, 67.2, 46.1, 44.4, 39.5, 28.6, 25.1, 18.7. HRMS-ESI: *m*/*z* calcd for $C_{15}H_{20}NO_3$ [M + H^+] 262.1438; found 262.1434. This material was used directly in the next step without any further purification.

Enzymatic aldol reactions. Analytical scale reactions (360 μL total volume) were conducted in capped 2 mL test tubes stirred with a vortex mixer (VIBRAX VXR basic, Ika) at 1000 rpm and 4 °C. Aldehydes (*S*)-**1a**, (*R*)-**1a** and (*rac*)-**1b** (24.5 μmol) were dissolved in dimethylformamide (72 μL) and mixed with a sodium borate solution (47.2 μL of 1.52 M, pH 7.0), a freshly

neutralized (pH 6.9–7.0) DHAP solution (141 μL, 14.4 μmol), and the aldolase (for RhuA catalyzed reactions: 100 μL, 0.19 mg of protein, 0.72 U corresponding to 2 U mL^{-1} reaction; for reactions with FucA wild-type or FucA mutants: 100 μL, 0.29 mg of protein, corresponding to 2.9 U FucA wild-type (8 U mL^{-1}), 0.029 U FucA F131A (0.08 U mL^{-1}), 0.62 U FucA F206A (1.74 U mL^{-1}), and 0.014 U FucA F131A/F206A (0.04 U mL^{-1})) was added to start the aldol reaction. Conversions were measured at 24 h of reaction time. Reaction monitoring was done as follows: samples (25 μL) were withdrawn at several reaction times, diluted with methanol (1000 μL) and analyzed by HPLC under the conditions described above. In parallel, samples (25 μL) were mixed with a solution (25 μL) of acid phosphatase (5.3 U mL^{-1} in sodium citrate buffer 400 mM, pH 4.5) and incubated for 24 h. After dilution with methanol (975 μL), samples were analyzed by HPLC.

Preparative enzymatic aldol additions. Reactions at preparative scale (20–40 mL total volume) were performed in 100 mL Erlenmeyer flasks with screw caps. Aldehydes (*S*)-**1a** (1.7 mmol), (*R*)-**1a** (2.12 mmol) and (*rac*)-**1c** (3.4 mmol) (85 mM final concentration) were dissolved in DMF (the amount corresponding to 20% v/v of the total), and sodium borate buffer (1.0 M, pH = 7.0, 20% v/v of the total) was added. Then, the DHAP solution (volume corresponding to 60% v/v of the total, 50 mM final concentration, 1.7 equiv. per mol of aldehyde) at pH 6.9, freshly prepared as described above, was added dropwise while stirring at 4 °C, with a vortex mixer. Finally, RhuA (2 U mL^{-1} reaction mixture) was added and mixed again. The Erlenmeyer flask was placed on a horizontal shaking bath (200 rpm) at 4 °C. The reactions were monitored by HPLC. When the concentration of the aldol adduct was constant with time (1–3 days, 66–81%) the reaction was stopped by addition of MeOH (1.5 times the reaction volume). Then, methanol was evaporated and the aqueous solution washed with ethyl acetate to remove the unreacted N-protected amino aldehyde. The aqueous layer was collected, and the remaining ethyl acetate removed under reduced pressure and lyophilized. The solid obtained was dissolved in plain water (*ca.* 20 mL) and the pH was adjusted to 5.5 with TFA. To this solution, acid phosphatase (5.3 U $mmol^{-1}$ phosphorylated adduct) was added. The reaction was followed by HPLC until no starting material was detected. Then, the reaction mixture was filtered through a 0.45 μm cellulose membrane filter. The filtrate was loaded onto an RP-XTerra® MS C_{18} 10 μm (19 × 250 mm) column, and eluted with a gradient of CH_3CN (8 to 56% over 30 min) in plain water. Pure fractions were pooled and lyophilized.

Removal of the Cbz group and reductive amination

The aldol adducts obtained (0.34–1.08 mmol) were dissolved in ethanol (5–10 mL), followed by the addition of plain water (20–50 mL). Pd/C (200 mg) was added. The reaction mixture was shaken under hydrogen (50 psi) overnight at room temperature. After removal of the catalyst by filtration through deactivated aluminum oxide, the pH of the filtrate was adjusted to pH 5.5 with formic acid (1 M), the solvent was removed under reduced pressure, and the product was lyophilized.

Purification by ion exchange chromatography

The polyhydroxylated indolizidine and quinolizidine derivatives **3a**, **3b**, **3c–e**, and **4a–f** were purified by ion exchange chromatography with an FPLC system by a procedure previously described by us.[13,14] CM-Sepharose CL-6B (Amersham Pharmacia) stationary phase in NH_4^+ form was packed into a glass column (450–25 mm) to provide a final bed volume of 220 mL. The flow rate was 4 mL min^{-1}. The CM-Sepharose-NH_4^+ was washed initially with H_2O. An aqueous solution of the crude material at pH 7 was then loaded onto the column. Minor colored impurities were washed away with H_2O (150 mL, 3 bed volumes). The retained compounds were eluted with aqueous NH_4OH (0.01 M): compounds **3a** and **3b** (load 100 mg): **3a**: elution volume, 256 mL (17.0 mg); **3b**: elution volume, 309 mL (21.3 mg); compounds **3c–3e** (load 40 mg): **3e**: elution volume, 120 mL (4.4 mg); **3d**: elution volume, 264 mL (14.0 mg); **3c**: elution volume, 408 mL (12.6 mg); compounds **4a–f** (load 242 mg), first elution with aqueous NH_4OH (0.005 M): **4d**: elution volume, 448 mL (57.6 mg); **4e**: elution volume, 840 mL (3.9 mg); further fractions from this run were pooled, lyophilized, and reloaded (134.5 mg), elution with aqueous NH_4OH (0.01 M): **4f**: elution volume, 560 mL (3.2 mg); **4b**/**4c**/**4f** mixture: elution volume, 608 mL (21.5 mg); **4b**/**4c** mixture: elution volume, 728 mL (14.1 mg); **4a**: elution volume, 1000 mL (23.1 mg). In each case, when necessary the operation was repeated until the whole crude sample was consumed. Pure fractions were pooled and lyophilized. Physical and NMR data are listed below. ^1H and ^{13}C NMR spectra scans and assignments are given in the ESI.†

(1*S*,2*S*,3*R*,8a*S*)-3-(Hydroxymethyl)octahydroindolizine-1,2-diol (3a). $[\alpha]_D^{22} = -76.8$ (*c* 1.9 in H_2O). ^1H NMR (600 MHz, D_2O) δ 4.04 (1H, dd, ^3J(H,H) = 7.4, 4.4 Hz), 3.75 (dd, ^3J(H,H) = 11.3, 7.3 Hz, 1H), 3.63 (dd, ^3J(H,H) = 11.4, 4.7 Hz, 1H), 3.51 (dd, ^3J(H,H) = 8.8, 4.4 Hz, 1H), 3.07 (d, ^3J(H,H) = 11.2 Hz, 1H), 2.54 (td, ^3J(H,H) = 7.2, 4.7 Hz, 1H), 1.97 (m, 1H), 1.87 (m, 2H), 1.74 (m, 1H), 1.59 (m, 1H), 1.37 (m, 1H), 1.19 (m, 2H). ^{13}C NMR (151 MHz, D_2O) 81.7, 75.3, 67.8, 67.7, 58.3, 52.1, 27.2, 23.8, 23.0. HRMS-ESI: *m*/*z* calcd for $C_9H_{17}NO_3$ 188.1287 [M + H^+]; found 188.1287.

(1*S*,2*S*,3*S*,8a*S*)-3-(Hydroxymethyl)octahydroindolizine-1,2-diol (3b). $[\alpha]_D^{22} = -3.5$ (*c* 2.0 in H_2O). ^1H NMR (600 MHz, D_2O) δ 3.86 (t, ^3J(H,H) = 4.8 Hz, 1H), 3.78 (dd, ^3J(H,H) = 12.1, 5.1 Hz, 1H), 3.71 (dd, ^3J(H,H) = 12.1, 5.1 Hz, 1H), 3.67 (dd, ^3J(H,H) = 7.4, 5.1 Hz, 1H), 2.98 (m, 1H), 2.92 (m, 1H), 2.68 (m, 1H), 2.60 (t, ^3J(H,H) = 10.5 Hz, 1H), 1.79 (m, 1H), 1.70 (m, 1H), 1.55 (m, 1H), 1.43 (m, 1H), 1.24 (m, 2H). ^{13}C NMR (151 MHz, D_2O): 80.6, 78.5, 67.5, 64.4, 59.5, 46.9, 26.6, 22.8, 22.1. HRMS-ESI: *m*/*z* calcd for $C_9H_{17}NO_3$: 188.1287 [M + H^+]; found 188.1285.

(1*R*,2*S*,3*R*,8a*R*)-3-(Hydroxymethyl)octahydroindolizine-1,2-diol (3c). $[\alpha]_D^{22} = -8.7$ (*c* 1.2 in H_2O). ^1H NMR (600 MHz, D_2O) δ 4.39 (t, ^3J(H,H) = 6.4 Hz, 1H), 3.87 (t, ^3J(H,H) = 5.7 Hz, 1H), 3.83 (dd, ^3J(H,H) = 12.2, 5.0 Hz, 1H), 3.77 (dd, ^3J(H,H) = 12.2, 5.5 Hz, 1H), 3.41 (m, 1H), 3.02 (m, 1H), 2.97 (s, 1H), 2.83 (t, ^3J(H,H) = 10.0 Hz, 1H), 1.80 (m, 1H), 1.70 (m, 1H), 1.57 (m, 1H), 1.50 (m, 2H), 1.30 (m, 3H). ^{13}C NMR (151 MHz, D_2O)

δ 73.6, 69.7, 64.2, 63.7, 57.8, 47.1, 25.3, 21.5, 21.3. HRMS-ESI: *m/z* calcd for $C_9H_{17}NO_3$ 188.1287 [M + H^+]; found 188.1288.

(1*S*,2*S*,3*S*,8a*R*)-3-(Hydroxymethyl)octahydroindolizine-1,2-diol (3d). $[\alpha]_D^{22}$ = +10.3 (*c* 1.3 in H_2O). ^{1}H NMR (600 MHz, D_2O) δ 3.84 (d, ^3J(H,H) = 4.2 Hz, 1H), 3.74 (d, ^3J(H,H) = 5.4 Hz, 1H), 3.72 (dd, ^3J(H,H) = 11.9, 5.4 Hz, 1H), 3.66 (dd, ^3J(H,H) = 11.9, 5.6 Hz, 1H), 3.18 (m, 1H), 2.32 (m, 1H), 2.25 (m, 1H), 2.06 (t, *J* = 11.2 Hz, 1H), 1.76 (m, 1H), 1.61 (t, ^3J(H,H) = 14.4 Hz, 2H), 1.38 (m, 2H), 1.28 (m, 1H). ^{13}C NMR (151 MHz, D_2O) δ 79.5, 77.8, 73.4, 67.5, 60.9, 52.5, 23.8, 23.8, 23.1. HRMS-ESI: *m/z* calcd for $C_9H_{17}NO_3$ 188.1287 [M + H^+]; found 188.1285.

(1*R*,2*S*,3*S*,8a*R*)-3-(Hydroxymethyl)octahydroindolizine-1,2-diol (3e). $[\alpha]_D^{22}$ = +37.9 (*c* 0.48 in H_2O). ^{1}H NMR (600 MHz, D_2O) δ 3.81 (dd, *J* = 7.0, 4.7 Hz, 1H), 3.67 (dd, ^3J(H,H) = 11.6, 5.1 Hz, 1H), 3.59 (dd, ^3J(H,H) = 11.6, 6.0 Hz, 1H), 3.49 (dd, ^3J(H,H) = 9.2, 7.1 Hz, 1H), 3.11 (d, ^3J(H,H) = 10.7 Hz, 1H), 2.30 (dd, ^3J(H,H) = 10.5, 5.1 Hz, 1H), 2.08 (m, 1H), 2.03 (m, 1H), 1.87 (m, 1H), 1.73 (m, 2H), 1.60 (m, 2H), 1.37 (m, 2H), 1.18 (m, 3H). ^{13}C NMR (151 MHz, D_2O) δ 73.3, 73.1, 70.7, 67.6, 60.9, 52.0, 27.5, 24.1, 23.0. HRMS-ESI: *m/z* calcd for $C_9H_{17}NO_3$ 188.1287 [M + H^+]; found 188.1284.

(2*S*,3*S*,4*R*,9a*S*)-4-(Hydroxymethyl)octahydro-1*H*-quinolizine-2,3-diol (4a). $[\alpha]_D^{22}$ = −36.1 (*c* 1.6 in H_2O) of the mixture. ^{1}H NMR (600 MHz, D_2O) δ 3.80 (m, 1H), 3.79 (m, 1H), 3.77 (m, 1H), 3.09 (d, ^3J(H,H) = 11.6 Hz, 1H), 2.45 (s, 1H), 2.30 (t, ^3J(H,H) = 10.8 Hz, 1H), 1.96 (t, ^3J(H,H) = 11.4 Hz, 1H), 1.77 (m, 1H), 1.63 (d, ^3J(H,H) = 12.3 Hz, 1H), 1.51 (m, 1H), 1.44 (m, 1H), 1.24 (m, 1H). ^{13}C NMR (151 MHz, D_2O) δ 70.3, 67.2, 62.0, 61.3, 56.2, 51.2, 33.7, 32.0, 24.7, 23.4. HRMS-ESI: *m/z* calcd for $C_{10}H_{19}NO_3$ 202.1443 [M + H^+]; found 202.1446.

Mixture 4b : 4f : 4c 70 : 9 : 21 $[\alpha]_D^{22}$ = −25.3 (*c* 1.7 in H_2O) of the mixture. NMR data for product (2*R*,3*S*,4*R*,9a*S*)-4-(hydroxymethyl)octahydro-1*H*-quinolizine-2,3-diol (4b). ^{1}H NMR (600 MHz, D_2O) δ 3.96 (s, 1H), 3.84 (m, 1H), 3.78 (dd, ^3J(H,H) = 11.7, 5.7 Hz, 1H), 3.68 (m, 1H), 3.17 (m, 1H), 2.35 (m, 1H), 2.23 (m, 1H), 2.05 (t, ^3J(H,H) = 11.2 Hz, 1H), 1.65 (m, 1H), 1.64 (m, 6H), 1.63 (m, 6H), 1.47 (m, 1H), 1.30 (m, 3H), 1.28 (m, 3H). ^{13}C NMR (151 MHz, D_2O) δ 69.9, 68.7, 66.2, 61.0, 60.9, 51.3, 34.0, 31.7, 24.6, 22.9. HRMS-ESI: *m/z* calcd for $C_{10}H_{19}NO_3$ 202.1443 [M + H^+]; found 202.1447.

Mixture 4c : 4b 62 : 38. NMR data for product (2*S*,3*S*,4*S*,9a*S*)-4-(hydroxymethyl)octahydro-1*H*-quinolizine-2,3-diol (4c). ^{1}H NMR (600 MHz, D_2O) δ 3.85 (m, 1H), 3.72 (m, 1H), 3.35 (t, ^3J(H,H) = 8.5 Hz, 1H), 3.18 (s, 1H), 3.04 (m, 1H), 2.93 (m, 1H), 2.68 (td, ^3J(H,H) = 13.7, 2.8 Hz, 1H), 1.81 (m, 1H), 1.79 (m, 1H), 1.71 (m, 1H), 1.59 (m, 1H), 1.53 (m, 1H), 1.45 (m, 1H), 1.35 (m, 1H), 1.32 (m, 1H). ^{13}C NMR (151 MHz, D_2O) δ 71.8, 68.6, 58.6, 57.1, 56.1, 49.1, 34.9, 24.5, 24.1, 18.4. HRMS-ESI: *m/z* calcd for $C_{10}H_{19}NO_3$ 202.1443 [M + H^+]; found 202.1449.

(2*S*,3*S*,4*S*,9a*R*)-4-(Hydroxymethyl)octahydro-1*H*-quinolizine-2,3-diol (4d). $[\alpha]_D^{22}$ = +18.8 (*c* 2.2 in H_2O). ^{1}H NMR (600 MHz, D_2O) δ 3.88 (dd, ^3J(H,H) = 12.8, 2.1 Hz, 1H), 3.70 (dd, ^3J(H,H) = 12.7, 2.9 Hz, 1H), 3.42 (ddd, ^3J(H,H) = 11.9, 9.3, 5.1 Hz, 1H), 3.17 (dd, ^3J(H,H) = 19.2, 9.9 Hz, 2H), 2.03 (t, ^3J(H,H) = 9.9 Hz, 1H), 1.86 (s, 2H), 1.80 (ddd, ^3J(H,H) = 12.8, 4.8, 2.0 Hz, 1H), 1.57 (m, 3H), 1.34 (m, 1H), 1.17 (m, 3H). ^{13}C NMR (151 MHz, D_2O) δ 72.6, 72.4, 68.8, 59.8, 58.2, 51.2, 38.5, 32.1, 24.7, 23.6. HRMS-ESI: *m/z* calcd for $C_{10}H_{19}NO_3$ 202.1443 [M + H^+]; found 202.1441.

(2*S*,3*S*,4*R*,9a*R*)-4-(Hydroxymethyl)octahydro-1*H*-quinolizine-2,3-diol (4e). $[\alpha]_D^{22}$ = −14.3 (*c* 0.28 in H_2O). ^{1}H NMR (600 MHz, D_2O) δ 3.92 (m, 2H), 3.86 (m, 1H), 3.85 (m, 1 H), 2.92 (brs, 1H), 2.74 (brs, 1H), 2.67 (brs, 2H), 1.76–1.30 (brs, 6H). ^{13}C NMR (151 MHz, D_2O) δ 69.7, 66.9, 55.9, 51.4, 37.4, 31.7. HRMS-ESI: *m/z* calcd for $C_{10}H_{19}NO_3$ 202.1443 [M + H^+]; found 202.1450.

(2*R*,3*S*,4*S*,9a*R*)-4-(Hydroxymethyl)octahydro-1*H*-quinolizine-2,3-diol (4f). $[\alpha]_D^{22}$ = −30.2 (*c* 0.32 in H_2O). ^{1}H NMR (600 MHz, D_2O) δ 3.99 (t, ^3J(H,H) = 13.1 Hz, 1H), 3.92 (m, 3H), 3.74 (dd, ^3J(H,H) = 12.8, 2.8 Hz, 1H), 3.26 (m, 1H), 2.36 (t, ^3J(H,H) = 10.7 Hz, 1H), 2.30 (d, ^3J(H,H) = 10.0 Hz, 1H), 2.02 (t, ^3J(H,H) = 11.9 Hz, 1H), 1.72 (m, 2H), 1.65 (m, 3H), 1.51 (m, 4H), 1.41 (m, 3H), 1.26 (m, 2H), 1.17 (m, 1H). ^{13}C NMR (151 MHz, D_2O) δ 68.2, 67.2, 64.0, 57.8, 55.6, 51.0, 36.8, 31.7, 24.4, 23.3. HRMS-ESI: *m/z* calcd for $C_{10}H_{19}NO_3$ 202.1443 [M + H^+]; found 202.1442.

Inhibitory activity assays

Enzymatic inhibition assays on commercial glycosidases, the kinetics of the inhibition, preparation of gut mucosal suspension and the inhibition assays on rat intestinal disaccharidases were performed as described in previous work.[13] The experimental details are summarized in the ESI.†

α-Amylase activity. This activity was assayed on α-amylase from porcine pancreas type I-A (A6255 Sigma-Aldrich) and α-amylase from human saliva type XIIIA (A1031 Sigma-Aldrich) using the Dahlqvist method and the starch azure assay. For the Dahlqvist method the activity was assayed in the same way as described for the mucosa (see ESI†). In this case, 30 U mL^{-1} of α-amylase from porcine pancreas (95 μL) or 2 U mL^{-1} of α-amylase from human saliva (95 μL) was used. Each product was tested at concentrations ranging from 0.2 nM to 1 mM in the presence of 4 g L^{-1} starch. For the starch-azure assay the reaction was carried out at 37 °C during 15 min in a total volume of 5 mL. The reaction mixture contained sodium phosphate buffer (18 mM Na_3PO_4, 45 mM NaCl, pH 7), starch azure (4.5 mL, 1.8% w/v), α-amylase from porcine pancreas (0.125 mg, 0.5 mL) and the inhibitor (1 mM, 50 μL). After 15 min the suspension was filtered through cellulose filter Whatman 54 and the absorbance of the filtrate was measured spectrophotometrically at 595 nm. The absorbance was proportional to the activity of the enzyme.

Amyloglucosidase activity. The activity of amyloglucosidase was assayed on amyloglucosidase from *Aspergillus niger* in a total volume of 100 μL, containing acetic buffer (10 mM, pH 5) using *p*-nitrophenyl-α-D-glucopyranoside (5 mM) as the substrate and amyloglucosidase (28.8 U mL^{-1}). Each potential inhibitor

was tested at concentrations ranging from 0.2 nM to 2 mM. The enzyme (20 μL) was pre-incubated in the presence of each product (1 μL) at 45 °C during 5 min. The reaction starts after the addition of the substrate (20 μL) at 45 °C. After 20 min the reaction was stopped by the addition of Tris–HCl 1 M (200 μL). The absorbance of the *p*-nitrophenol released at 405 nm is proportional to the enzyme activity.

Starch digestion activity. Starch digestion activity was determined by colorimetric measurement of the glucose release by the action of brush border enzymes on starch, according to the Dahlqvist method. Diluted homogenized mucosa (95 μL) in phosphate buffer pH 6.8 (300 μL) was preincubated during 30 min at 37 °C with the inhibitor (5 μL, to final concentrations ranging from 0.2 nM to 1 mM). Then starch was added (100 μL, 4 g L^{-1} substrate), and the mixture was incubated at 37 °C during 30 min with gentle shaking (250 rpm). The total volume was 500 μL. The reaction was terminated after 30 min by the addition of Glucostat solution (2 mL, Tris 0.5 M, 4-hydroxybenzoic acid 10 mM, 4-aminoantipyrine 0.4 mM, glucose oxidase 1480 U L^{-1}, peroxidase 250 U L^{-1}, pH 7.3). After further incubation (2 h at 37 °C) the amount of glucose was measured at 505 nm using an ELISA reader and 96-well plates. Activity (μmol of substrate hydrolyzed per hour) was normalized to protein content evaluated by the Bradford method. Starch digestion activity in the absence of inhibitor was 20.79 ± 2.39 μmol glucose L^{-1} h^{-1} mg^{-1} protein. Each product was tested on the mucosa of five rats and each mucosa was assayed in triplicate.

Minimum inhibitory concentration (MIC) determination. REMA plate method. Mycobacteria strain (*M. tuberculosis* H37Rv laboratory strain). The resazurin microtiter assay (REMA) plate method[29] was performed in Middlebrook 7H9 Broth medium supplemented with 0.2% glycerol, 0.5% albumin-dextrose catalase (Becton Dickinson) and 0.05% Tween 80 (7H9-S). Resazurin sodium salt powder (Sigma-Aldrich 199303-1G) was prepared at 0.01% w/v concentration in distilled water and sterilized by filtration through a 0.2 μm membrane. The inoculum was prepared as follows: *M. tuberculosis* H37Rv Pasteur was grown in 250 mL PYREX bottles in a shaking incubator at 37 °C and 120 rpm in 7H9-S, it was left to grow to mid-log phase, and stored at −70 °C. The inoculum was prepared by diluting an aliquot (3 mL) of the previous solution down to 10^6 CFU mL^{-1} in 7H9-S.

Serial two-fold dilutions of each inhibitor in 7H9-S medium (100 μL) were prepared directly in 96-well plates at concentrations ranging from 3 mg mL^{-1} to 0.094 mg mL^{-1} for **3a**, **3b**, **3c**, and **3e** inhibitors and from 0.75 mg mL^{-1} to 0.012 mg mL^{-1} for **4e**, **4f** and LAB (**9**). Growth controls containing no antibiotic, sterility controls without inoculation and inhibition controls containing isoniazide (1 μg mL^{-1}) were also included in the assay.

The assay was conducted as follows. The inoculum (100 μL) was added to the wells containing the inhibitors and to the corresponding control assays, the plates were covered, sealed, and incubated at 37 °C in a standard atmosphere. After 6 days of incubation, resazurin solution (100 μL) was added to each well, incubated during 2 days at 37 °C, and assessed for color development. A change from blue to pink indicates reduction of resazurin and therefore bacterial growth. The MIC was defined as the lowest drug concentration that prevented this color change. Experiments were performed in triplicate.

Computational methods

All calculations were carried out with the package Schrödinger Suite 2011[39] through its graphical interphase Maestro.[40] Compounds **3a–4f**, DOC and DOEC were modeled in their neutral state. Conformational searches were carried out using the mixed MCMM/LMCS method[41] implemented in the program MacroModel,[42] with the default force field OPLS 2005, an enhanced version of the OPLSAA all atom force field[43] developed by Schrödinger to provide a larger coverage of organic functionality. All the minimum energy conformers detected within 5.0 kcal mol^{-1} from the lowest energy minimum for each compound were subjected to further minimization through density functional theory calculations at the B3LYP/6-31G** level,[44] under water solvation conditions, with the program Jaguar.[45] Water solvation was implemented by using the standard Poisson–Boltzmann solver[46] included in Jaguar. Further single point calculations were carried out at the B3LYP/cc-pVTZ(-f) level[47] to recalculate the energies in solution and to calculate the vibrational frequencies, the zero-point energies (ZPE) and the thermal and entropic corrections at 298.15 °K. Boltzmann contributions for each conformation were determined from the relative free energies in solution (ΔG^{wat}). Most of these calculation steps were carried out through a Knime workflow[48,49] that uses Schrödinger Knime extensions to perform (1) the conformational search, (2) the DFT minimization, and (3) the single point DFT calculation automatically over a collection of structures.

Acknowledgements

This work was supported by the Spanish MICINN CTQ2009–07359 and CTQ2009–08328, Generalitat de Catalunya (2009 SGR 00281), and ESF project COST CM0701. X. Garrabou acknowledges the CSIC for the I3P predoctoral scholarship and L. Gomez acknowledges Generalitat de Catalunya and Bioglane S.L.N.E. for the predoctoral contract.

References

1 A. D. Elbein, R. Solf, P. R. Dorling and K. Vosbeck, *Proc. Natl. Acad. Sci. U. S. A.*, 1981, **78**, 7393–7397; N. Asano, T. Yamashita, K. Yasuda, K. Ikeda, H. Kizu, Y. Kameda, A. Kato, R. J. Nash, H. S. Lee and K. S. Ryu, *J. Agric. Food Chem.*, 2001, **49**, 4208–4213; N. Asano, *Curr. Top. Med. Chem.*, 2003, **3**, 471–484; P. Greimel, J. Spreitz, A. E. Stutz and T. M. Wrodnigg, *Curr. Top. Med. Chem.*, 2003, **3**, 513–523; J. P. Michael, *Nat. Prod. Rep.*, 2008, **25**, 139–165; N. Asano, in *Modern Alkaloids: Structure, Isolation, Synthesis and Biology*, ed. E. Fattorusso and O. Taglialatela-Scafati, Wiley-VCH, Weinheim, 2008, pp. 111–138; N. Asano and H. Hashimoto, in *Glycoscience: Chemistry and Chemical Biology*, ed. B. O. Fraser-Reid, K. Tatsuta and J. Thiem, Springer, Berlin, 2nd edn, 2008, vol. 3, pp. 1887–1911; B. G. Winchester, *Tetrahedron: Asymmetry*, 2009, **20**, 645–651; X. G. Hu, B. Bartholomew, R. J. Nash, F. X. Wilson, G. W. J. Fleet, S. Nakagawa, A. Kato, Y. M. Jia, R. van Well and C. Y. Yu, *Org. Lett.*, 2010, **12**, 2562–2565; G. Gradnig, A. Berger, V. Grassberger, A. E. Stütz and G. Legler, *Tetrahedron Lett.*, 1991, **32**, 4889–4892.
2 A. E. Stutz, *Iminosugars as Glycosidase Inhibitors: Nojirimycin and Beyond*, Wiley-VCH, Weinheim, 1999.
3 A. Bastida, A. Fernandez-Mayoralas, R. G. Arrayas, F. Iradier, J. C. Carretero and E. Garcia-Junceda, *Chem.–Eur. J.*, 2001, **7**, 2390–2397;

From Synthesis Iminosugars to Therapeutic Applications, ed. P. Compain and O. R. Martin, John Wiley & Sons Ltd, Sussex, England, 2007; W. H. Pearson and E. J. Hembre, *J. Org. Chem.*, 1996, **61**, 5546–5556.
4 W. H. Pearson and E. J. Hembre, *J. Org. Chem.*, 1996, **61**, 5537–5545.
5 V. Ratovelomanana, L. Vidal, J. Royer and H. P. Husson, *Heterocycles*, 1991, **32**, 879–888; C. R. Johnson and B. A. Johns, *Tetrahedron Lett.*, 1997, **38**, 7977–7980; J. C. Carretero, R. G. Arrayás and I. S. de Gracia, *Tetrahedron Lett.*, 1997, **38**, 8537–8540; J. C. Carretero and R. G. Arrayas, *J. Org. Chem.*, 1998, **63**, 2993–3005; G. Rassu, P. Carta, L. Pinna, L. Battistini, F. Zanardi, D. Acquotti and G. Casiraghi, *Eur. J. Org. Chem.*, 1999, 1395–1400; P. Gebarowski and W. Sas, *Chem. Commun.*, 2001, 915–916; A. T. Carmona, J. Fuentes and I. Robina, *Tetrahedron Lett.*, 2002, **43**, 8543–8546; F. M. Cordero, F. Pisaneschi, M. Gensini, A. Goti and A. Brandi, *Eur. J. Org. Chem.*, 2002, 1941–1951; S. H. L. Verhelst, B. Paez Martinez, M. S. M. Timmer, G. Lodder, G. A. van der Marel, H. S. Overkleeft and J. H. van Boom, *J. Org. Chem.*, 2003, **68**, 9598–9603; D. D. Dhavale, S. M. Jachak, N. P. Karche and C. Trombini, *Tetrahedron*, 2004, **60**, 3009–3016; D. D. Dhavale, S. M. Jachak, N. P. Karche and C. Trombini, *Synlett*, 2004, 1549–1552; D. Socha, K. Pasniczek, M. Jurczak, J. Solecka and M. Chmielewski, *Carbohydr. Res.*, 2006, **341**, 2005–2011; L. Song, E. N. Duesler and P. S. Mariano, *J. Org. Chem.*, 2004, **69**, 7284–7293; K. Pasniczek, D. Socha, M. Jurczak, J. Solecka and M. Chmielewski, *Can. J. Chem.*, 2006, **84**, 534–539; F. Cardona, A. Goti and A. Brandi, *Eur. J. Org. Chem.*, 2007, **2007**, 1551–1565; G. Lesma, A. Colombo, N. Landoni, A. Sacchetti and A. Silvani, *Tetrahedron: Asymmetry*, 2007, **18**, 1948–1954; T. Muramatsu, S. Yamashita, Y. Nakamura, M. Suzuki, N. Mase, H. Yoda and K. Takabe, *Tetrahedron Lett.*, 2007, **48**, 8956–8959; M.-J. Chen and Y.-M. Tsai, *Tetrahedron Lett.*, 2007, **48**, 6271–6274; K. Paśniczek, M. Jurczak, J. Solecka, Z. Urbańczyk-Lipkowska and M. Chmielewski, *J. Carbohydr. Chem.*, 2007, **26**, 195–211; X.-P. Jiang, Y. Cheng, G.-F. Shi and Z.-M. Kang, *J. Org. Chem.*, 2007, **72**, 2212–2215; G.-F. Shi, J.-Q. Li, X.-P. Jiang and Y. Cheng, *Tetrahedron*, 2008, **64**, 5005–5012; S. Chandrasekhar, B. V. D. Vijaykumar and T. V. Pratap, *Tetrahedron: Asymmetry*, 2008, **19**, 746–750; R. Azzouz, C. Fruit, L. Bischoff and F. Marsais, *J. Org. Chem.*, 2008, **73**, 1154–1157; M. A. Alam and Y. D. Vankar, *Tetrahedron Lett.*, 2008, **49**, 5534–5536; J. A. Tamayo, F. Franco, D. Lo Re and F. Sanchez-Cantalejo, *J. Org. Chem.*, 2009, **74**, 5679–5682; X. Li, Z. Zhu, K. Duan, H. Chen, Z. Li, Z. Li and P. Zhang, *Tetrahedron*, 2009, **65**, 2322–2328; B. Macchi, A. Minutolo, S. Grelli, F. Cardona, F. M. Cordero, A. Mastino and A. Brandi, *Glycobiology*, 2010, **20**, 500–506; L. Gang, W. Tian-Jun, R. Yuan-Ping and H. Pei-Qiang, *Chem.–Eur. J.*, 2010, **16**, 5755–5768; I. Delso, T. Tejero, A. Goti and P. Merino, *Tetrahedron*, 2010, **66**, 1220–1227; S. Chooprayoon, C. Kuhakarn, P. Tuchinda, V. Reutrakul and M. Pohmakotr, *Org. Biomol. Chem.*, 2011, **9**, 531–537; S. N. Murthy and Y. V. D. Nageswar, *Synthesis*, 2011, **2011**, 755–758; D. J. Wardrop and E. G. Bowen, *Org. Lett.*, 2011, **13**, 2376–2379.
6 K. S. A. Kumar, V. D. Chaudhari and D. D. Dhavale, *Org. Biomol. Chem.*, 2008, **6**, 703–711.
7 P. S. Liu, R. S. Rogers, M. S. Kang and P. S. Sunkara, *Tetrahedron Lett.*, 1991, **32**, 5853–5856.
8 P. Zhou, H. M. Salleh and J. F. Honek, *J. Org. Chem.*, 1993, **58**, 264–266.
9 A. Brandi, S. Cicchi, F. M. Cordero, R. Frignoli, A. Goti, S. Picasso and P. Vogel, *J. Org. Chem.*, 1995, **60**, 6806–6812.
10 M. S. Kang, P. S. Liu, R. C. Bernotas, B. S. Harry and P. S. Sunkara, *Glycobiology*, 1995, **5**, 147–152; B. Davis, A. A. Bell, R. J. Nash, A. A. Watson, R. C. Griffiths, M. G. Jones, C. Smith and G. W. J. Fleet, *Tetrahedron Lett.*, 1996, **37**, 8565–8568; A. T. Carmona, J. Fuentes, I. Robina, E. Rodriguez Garcia, R. Demange, P. Vogel and A. L. Winters, *J. Org. Chem.*, 2003, **68**, 3874–3883; F. Cardona, G. Moreno, F. Guarna, P. Vogel, C. Schuetz, P. Merino and A. Goti, *J. Org. Chem.*, 2005, **70**, 6552–6555; N. Langlois, B. K. Le Nguyen, P. Retailleau, C. Tarnus and E. Salomon, *Tetrahedron: Asymmetry*, 2006, **17**, 53–60; T. Ayad, Y. Genisson and M. Baltas, *Org. Biomol. Chem.*, 2005, **3**, 2626–2631; D. Baumann, K. Bennis, I. Ripoche, V. Théry and Y. Troin, *Eur. J. Org. Chem.*, 2008, **2008**, 5289–5300; M. A. Alam, A. Kumar and Y. D. Vankar, *Eur. J. Org. Chem.*, 2008, **2008**, 4972–4980; A. E. Hakansson, J. van Ameijde, G. Horne, R. J. Nash, M. R. Wormald, A. Kato, G. S. Besra, S. Gurcha and G. W. J. Fleet, *Tetrahedron Lett.*, 2008, **49**, 179–184.
11 C. Schaller and P. Vogel, *Helv. Chim. Acta*, 2000, **83**, 193–232; N. Kumari and Y. D. Vankar, *Org. Biomol. Chem.*, 2009, **7**, 2104–2109; G. Pandey, D. Grahacharya, K. S. Shashidhara, M. I. Khan and V. G. Puranik, *Org. Biomol. Chem.*, 2009, **7**, 3300–3307.
12 J. Calveras, J. Casas, T. Parella, J. Joglar and P. Clapés, *Adv. Synth. Catal.*, 2007, **349**, 1661–1666.
13 X. Garrabou, L. Gomez, J. Joglar, S. Gil, T. Parella, J. Bujons and P. Clapés, *Chem.–Eur. J.*, 2010, **16**, 10691–10706.
14 J. Calveras, M. Egido-Gabás, L. Gómez, J. Casas, T. Parella, J. Joglar, J. Bujons and P. Clapés, *Chem.–Eur. J.*, 2009, **15**, 7310–7328.
15 L. Gómez, E. Molinar-Toribio, M. Á. Calvo-Torras, C. Adelantado, M. E. Juan, J. M. Planas, X. Cañas, C. Lozano, S. Pumarola, P. Clapés and J. L. Torres, *Br. J. Nutr.*, 2012, **107**, 1739–1746.
16 R. Eskandari, K. Jones, K. Ravinder Reddy, K. Jayakanthan, M. Chaudet, D. R. Rose and B. M. Pinto, *Chem.–Eur. J.*, 2011, **17**, 14817–14825.
17 A. Ceriello, *Diab. Vasc. Dis. Res.*, 2008, **5**, 260–268; R. R. Holman, C. A. Cull and R. C. Turner, *Diabetes Care*, 1999, **22**, 960–964.
18 M. Cho, J. H. Han and S. You, *LWT–Food Sci. Technol.*, 2011, **44**, 1164–1171; J. Singh, A. Dartois and L. Kaur, *Trends Food Sci. Technol.*, 2010, **21**, 168–180.
19 N. T. Patil, J. N. Tilekar and D. D. Dhavale, *Tetrahedron Lett.*, 2001, **42**, 747–749; N. T. Patil, J. N. Tilekar and D. D. Dhavale, *J. Org. Chem.*, 2001, **66**, 1065–1074.
20 E. J. Hembre and W. H. Pearson, *Tetrahedron*, 1997, **53**, 11021–11032.
21 I. Pastuszak, R. J. Molyneux, L. F. James and A. D. Elbein, *Biochemistry*, 1990, **29**, 1886–1891.
22 *Evaluation of Enzyme Inhibitors in Drug Discovery: A Guide to Medicinal Chemists and Pharmacologists*, ed. R. A. Copeland, John Wiley & Sons, Hoboken, NJ, USA, 2005.
23 S. P. Sanap, S. Ghosh, A. M. Jabgunde, R. V. Pinjari, S. P. Gejji, S. Singh, B. A. Chopade and D. D. Dhavale, *Org. Biomol. Chem.*, 2010, **8**, 3307–3315.
24 K. M. Park and N. S. Wang, *Biotechnol. Tech.*, 1991, **5**, 205–208; H. Rinderknecht, P. Wilding and B. J. Haverback, *Experientia*, 1967, **23**, 805.
25 A. Dahlqvist, *Anal. Biochem.*, 1964, **7**, 18–25.
26 J. P. Shilvock, J. R. Wheatley, R. J. Nash, A. A. Watson, R. C. Griffiths, T. D. Butters, M. Muller, D. J. Watkin, D. A. Winkler and G. W. J. Fleet, *J. Chem. Soc., Perkin Trans. 1*, 1999, 2735–2745.
27 R. Lucas, P. Balbuena, J. C. Errey, M. A. Squire, S. S. Gurcha, M. McNeil, G. S. Besra and B. G. Davis, *ChemBioChem*, 2008, **9**, 2197–2199.
28 J. A. Maddry, N. Bansal, L. E. Bermudez, R. N. Comber, I. M. Orme, W. J. Suling, L. N. Wilson and R. C. Reynolds, *Bioorg. Med. Chem. Lett.*, 1998, **8**, 237–242.
29 J.-C. Palomino, A. Martin, M. Camacho, H. Guerra, J. Swings and F. Portaels, *Antimicrob. Agents Chemother.*, 2002, **46**, 2720–2722.
30 S.-H. Jung, J.-H. Jeong, P. Miller and C.-H. Wong, *J. Org. Chem.*, 1994, **59**, 7182–7184.
31 L. Vidal, O. Durany, T. Suau, P. Ferrer, M. D. Benaiges and G. Caminal, *J. Chem. Technol. Biotechnol.*, 2003, **78**, 1171–1179; X. Garrabou, J. Joglar, T. Parella, J. Bujons and P. Clapés, *Adv. Synth. Catal.*, 2011, **353**, 89–99.
32 O. Durany, G. Caminal, C. de Mas and J. Lopez-Santin, *Process Biochem.*, 2004, **39**, 1677–1684.
33 J. A. Castillo, J. Calveras, J. Casas, M. Mitjans, M. P. Vinardell, T. Parella, T. Inoue, G. A. Sprenger, J. Joglar and P. Clapés, *Org. Lett.*, 2006, **8**, 6067–6070; X. Garrabou, J. Calveras, J. Joglar, T. Parella, J. Bujons and P. Clapes, *Org. Biomol. Chem.*, 2011, **9**, 8430–8436; M. Gutierrez, T. Parella, J. Joglar, J. Bujons and P. Clapés, *Chem. Commun.*, 2011, **47**, 5762–5764.
34 J. R. Luly, J. F. Dellaria, J. J. Plattner, J. L. Soderquist and N. Yi, *J. Org. Chem.*, 1987, **52**, 1487–1492.
35 M. Ocejo, J. L. Vicario, D. Badia, L. Carrillo and E. Reyes, *Synlett*, 2005, 2110–2112.
36 D. Minato, Y. Nagasue, Y. Demizu and O. Onomura, *Angew. Chem., Int. Ed.*, 2008, **47**, 9458–9461; T. Gehring, J. Podlech and A. Rothenberger, *Synthesis*, 2008, **2008**, 2476–2487.
37 F. Sánchez-Sancho and B. Herradón, *Tetrahedron: Asymmetry*, 1998, **9**, 1951–1965.
38 A. Rouchaud and J.-C. Braekman, *Eur. J. Org. Chem.*, 2009, **2009**, 2666–2674; E. C. Carlson, L. K. Rathbone, H. Yang, N. D. Collett and R. G. Carter, *J. Org. Chem.*, 2008, **73**, 5155–5158.
39 Schrödinger, LLC, New York.
40 Maestro, version 9.2, Schrödinger, LLC, New York, NY, 2011.
41 I. Kolossvary and W. C. Guida, *J. Comput. Chem.*, 1999, **20**, 1671–1684.

42 MacroModel, version 9.9, Schrödinger, LLC, New York, NY, 2011.
43 W. L. Jorgensen, D. S. Maxwell and J. Tirado-Rives, *J. Am. Chem. Soc.*, 1996, **118**, 11225–11236.
44 A. D. Becke, *J. Chem. Phys.*, 1993, **98**, 5648–5652; C. Lee, W. Yang and R. G. Parr, *Phys. Rev. B: Condens. Matter*, 1988, **37**, 785–789.
45 Jaguar, version 7.8, Schrödinger, LLC, New York, NY, 2011.
46 D. J. Tannor, B. Marten, R. Murphy, R. A. Friesner, D. Sitkoff, A. Nicholls, B. Honig, M. Ringnalda and W. A. Goddard III, *J. Am. Chem. Soc.*, 1994, **116**, 11875–11882; B. Marten, K. Kim, C. Cortis, R. A. Friesner, R. B. Murphy, M. N. Ringnalda, D. Sitkoff and B. Honig, *J. Phys. Chem.*, 1996, **100**, 11775–11788.
47 T. H. Dunning Jr., *J. Chem. Phys.*, 1989, **90**, 1007–1023; R. A. Kendall, T. H. Dunning Jr. and R. J. Harrison, *J. Chem. Phys.*, 1992, **96**, 6796–6806; D. E. Woon and T. H. Dunning Jr., *J. Chem. Phys.*, 1993, **98**, 1358–1371; D. E. Woon and T. H. Dunning Jr., *J. Chem. Phys.*, 1994, **100**, 2975–2988.
48 Konstanz Information Miner, version 2.3.0.
49 M. R. Berthold, N. Cebron, F. Dill, T. R. Gabriel, T. Kötter, T. Meinl, P. Ohl, C. Sieb, K. Thiel and B. Wiswedel, *KNIME: The Konstanz Information Miner*, Springer, 2008.